Global statistical evidence for chorus as the embryonic source of plasmaspheric hiss

Nigel P. Meredith,[1] Richard B. Horne,[1] Jacob Bortnik,[2] Richard M. Thorne,[2] Lunjin Chen,[2] Wen Li,[2] and Angélica Sicard-Piet[3]

Received 2 May 2013; revised 23 May 2013; accepted 24 May 2013; published 18 June 2013.

[1] The origin of plasmaspheric hiss, the electromagnetic emission responsible for the gap between the inner and outer radiation belts, has been debated for over four decades. Recently, a new theory proposed that chorus, which is excited in the equatorial region outside the plasmapause, can propagate to low altitudes on the dayside and evolve into plasmaspheric hiss. Here we combine data from six satellites and show that chorus extends along the Earth's magnetic field to high latitudes in the prenoon sector, and, in the equatorial region, there is a clear gap of the order of 1–2 Earth radii between plasmaspheric hiss at $L^* < 4$ and chorus further out, consistent with ray tracing modeling from a chorus source. Our observations confirm two of the key predictions of the new theory and provide the first statistical evidence for chorus as the embryonic source of plasmaspheric hiss. **Citation:** Meredith, N. P., R. B. Horne, J. Bortnik, R. M. Thorne, L. Chen, W. Li, and A. Sicard-Piet (2013), Global statistical evidence for chorus as the embryonic source of plasmaspheric hiss, *Geophys. Res. Lett.*, *40*, 2891–2896, doi:10.1002/grl.50593.

1. Introduction

[2] Plasmaspheric hiss is a broadband, structureless, electromagnetic emission that tends to occur in the frequency range from 100 Hz to several kilohertz, with peak power near a few hundred hertz [*Thorne et al.*, 1973; *Meredith et al.*, 2007]. The waves are generally observed throughout the higher density regions associated with the Earth's plasmasphere [*Thorne et al.*, 1973] and plasmaspheric plumes [*Summers et al.*, 2008]. While the emission occurs at all magnetic local times and latitudes within the plasmasphere, there is a pronounced day-night asymmetry with the dayside emissions typically an order of magnitude larger than those on the nightside [*Meredith et al.*, 2004, 2006a]. Plasmaspheric hiss can persist during relatively quiet conditions, but the emission intensifies during storms and substorms [*Smith et al.*, 1974; *Thorne et al.*, 1974; *Meredith et al.*, 2004].

[1]British Antarctic Survey, Natural Environment Research Council, Cambridge, UK.
[2]Department of Atmospheric and Oceanic Sciences, University of California, Los Angeles, California, USA.
[3]Office National d'Etudes et de Recherches Aérospatiales, Toulouse, France.

Corresponding author: N. P. Meredith, British Antarctic Survey, Natural Environment Research Council, Madingley Road, Cambridge CB3 0ET, UK. (nmer@bas.ac.uk)

0094-8276/13/10.1002/grl.50593

[3] Plasmaspheric hiss is an important constituent of the Earth's magnetospheric plasma environment. Resonant pitch angle scattering of energetic electrons by plasmaspheric hiss largely accounts for the formation of the slot region between the inner and outer radiation belts [*Lyons and Thorne*, 1973; *Meredith et al.*, 2007, 2009]. Resonant wave particle interactions with plasmaspheric hiss also contribute to the loss of outer radiation belt electrons during the main and recovery phases of geomagnetic storms [*Summers et al.*, 2007] and the quiet time decay of energetic electrons in the outer radiation belt [*Meredith et al.*, 2006b; *Summers et al.*, 2007].

[4] Despite over 40 years of scientific research, the origin of plasmaspheric hiss has yet to be conclusively confirmed. The two potential mechanisms investigated in early studies were in situ growth of wave turbulence in space [*Thorne et al.*, 1973; *Church and Thorne*, 1983] and lightning-generated whistlers [*Sonwalkar and Inan*, 1989]. However, the former could not achieve the observed power levels [*Church and Thorne*, 1983], and the latter could not explain the lack of correlation between plasmaspheric hiss below 2 kHz and land mass [*Meredith et al.*, 2006a], where more lightning occurs, or the geomagnetic control of plasmaspheric hiss [*Meredith et al.*, 2004]. More recently, *Bortnik et al.* [2008] suggested that plasmaspheric hiss could originate from bursts of short duration (∼0.1 s) chorus emissions which are excited outside the plasmapause and then propagate into and become trapped inside the plasmapause. Case studies of a strong correlation between the amplitude modulation of chorus and plasmaspheric hiss on two Time History of Events and Macroscale Interactions during Substorms (THEMIS) spacecraft [*Bortnik et al.*, 2009] and two Cluster spacecraft [*Wang et al.*, 2011] together with dayside observations of downward propagating chorus and upward propagating plasmaspheric hiss by the Polar spacecraft [*Tsurutani et al.*, 2012] lend support to the new theory. While initial ray tracing modeling treating chorus as the source of plasmaspheric hiss alone underestimated the typical plasmaspheric hiss power by 10–20 dB [*Chen et al.*, 2012a, 2012b], many of the observational characteristics of plasmaspheric hiss were reproduced, including the observed frequency band, the geomagnetic control, and the day-night asymmetry in intensity. Later, the potential difficulty of underestimating the intensity of plasmaspheric hiss was resolved when cyclotron resonant wave growth inside the plasmapause was included in the modeling [*Chen et al.*, 2012c]. To test the new theory robustly we construct a global statistical model of the waves in the plasmaspheric hiss frequency range and look for statistical signatures of the relationship between plasmaspheric hiss and chorus.

Table 1. Format of the Wave Database

Parameter	Bins
Frequency	6 fixed frequency bands
L^*	90 linear steps from $L^* = 1$ to $L^* = 10$
MLT	24 linear steps from 0:00 MLT to 24:00 MLT
λ_m	60 linear steps from –90° to 90°
Activity	10 activity levels as monitored by *AE*

2. Instrumentation and Data Analysis

[5] To construct a comprehensive database of plasmaspheric hiss and associated chorus in the inner magnetosphere we combined data from six satellites. We used approximately 3 years of data from Dynamics Explorer 1, 10 years of data from Cluster 1, 1 year of data from Double Star TC-1, and 17 months of data from THEMIS A, D, and E. The instrumentation and data analysis techniques are described in detail in *Meredith et al.* [2012]. For the present study we binned the data from each satellite as a function of fixed frequency band, L^*, magnetic local time (MLT), magnetic latitude (λ_m), and geomagnetic activity as monitored by the *AE* index as detailed in Table 1. Here L^* is related to the third adiabatic invariant and may be thought of as the radial distance in Earth radii to the equatorial locus of the symmetric shell on which particles would be found if the non-dipolar components of the trapping field were adiabatically removed [*Roederer*, 1970]. For the database, L^* and MLT were computed using the Office National d'Etudes et de Recherches Aérospatiale Département Environnement Spatial ONERA-DESP library V4.2 (D. Boscher et al., ONERA DESP library V4.2 2008) with the International Geomagnetic Reference Field at the middle of the appropriate year and the Olson-Pfitzer quiet time model [*Olson and Pfitzer*, 1977]. The six fixed frequency bands chosen to capture the plasmaspheric hiss wave power were 100–200, 200–500, 500–1000, 1000–2000, 2000–3000, and 3000–4000 Hz. We then combined the data from each of the satellites, weighting the data from each individual satellite by the corresponding number of samples, to produce a com-

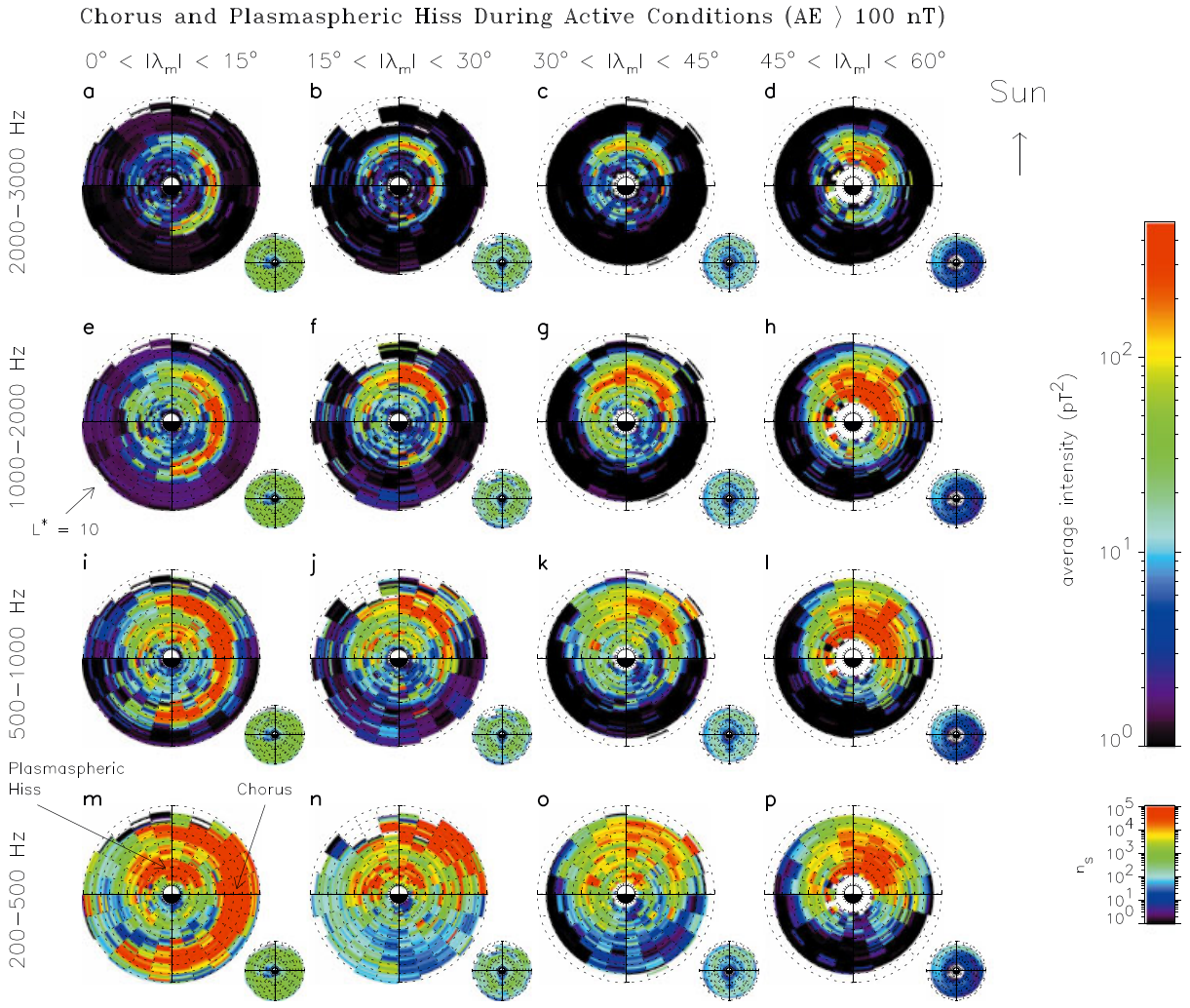

Figure 1. Global maps of the wave intensity as a function of L^* and MLT during active conditions (*AE* > 100 nT) for (from bottom to top) increasing wave frequency bands and (from left to right) increasing magnetic latitude. The plots extend linearly out to $L^* = 10$ with noon at the top and dawn to the right. The average intensities are shown in the large panels and the corresponding sampling distributions in the subpanels.

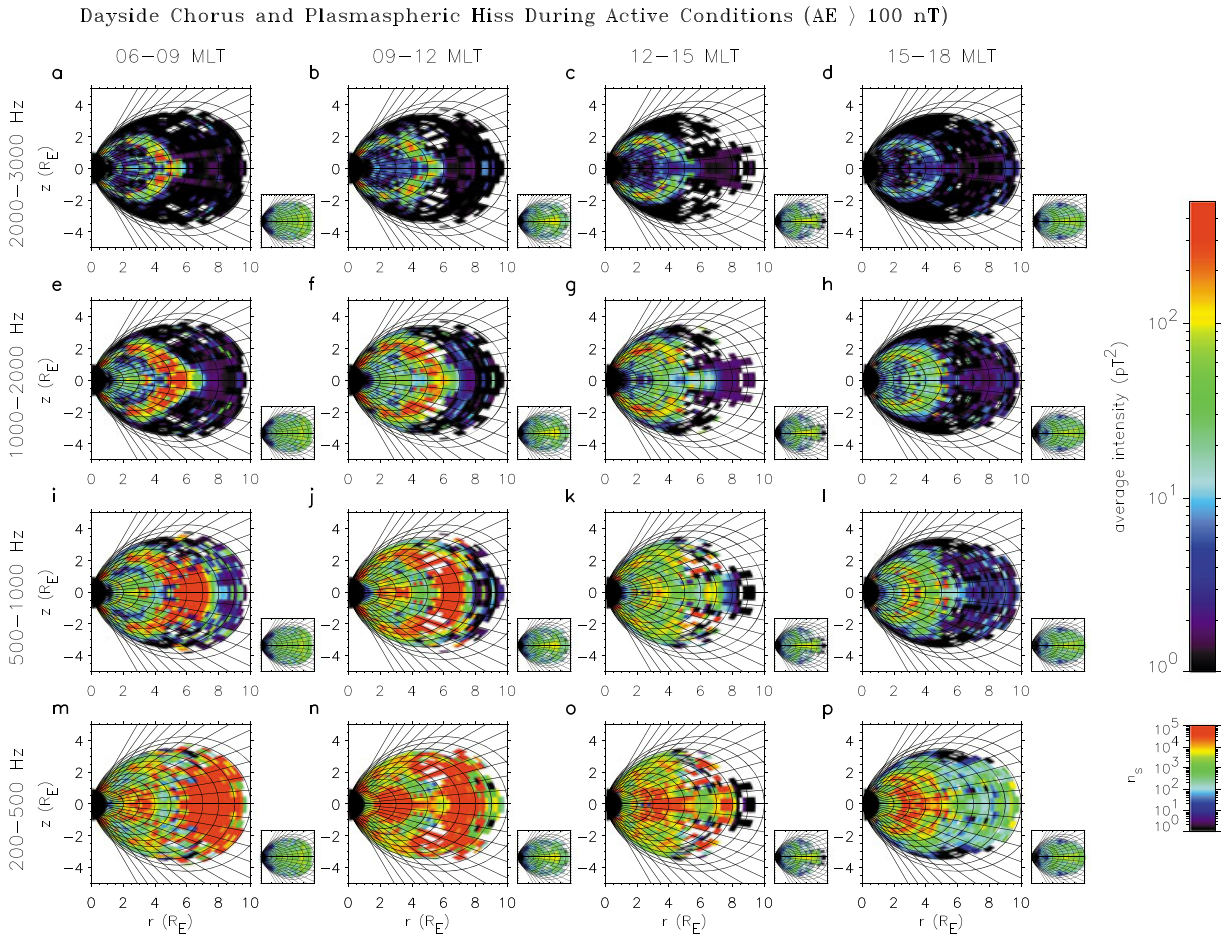

Figure 2. Global maps of the dayside wave intensity in the meridional plane during active conditions (AE > 100 nT) for (from bottom to top) increasing wave frequency bands and (from left to right) increasing magnetic local time. The average intensities are shown in the large panels and the corresponding sampling distributions in the subpanels.

bined wave database as a function of frequency band, L^*, MLT, λ_m, and geomagnetic activity.

3. Global Morphology

3.1. MLT Distribution

[6] The global distribution of waves in the plasmaspheric hiss frequency range during active conditions (AE > 100 nT) is shown as a function of frequency band, λ_m, L^*, and MLT in Figure 1. Each plot extends linearly out to L^* = 10 with noon at the top and dawn to the right. The average intensities are shown in the large panels and the corresponding sampling distributions in the small panels. The data have been averaged over both hemispheres into bins of width $0.2L^*$. Magnetosonic waves can potentially contaminate the observations when the wave frequency becomes less than the lower hybrid resonance frequency, but these waves are tightly confined to the magnetic equatorial plane [*Nemec et al.*, 2005]. We removed these waves to first order from the plots by excluding emissions below the lower hybrid frequency within ±3° of the magnetic equator.

[7] In the equatorial region, 0 < $|\lambda_m|$ < 15°, at low frequencies in the range 200–500 Hz, there are two distinct regions of intense waves, separated by a gap between L^* = 4 and 6 (Figure 1m). In the inner region, 2 < L^* < 4, enhanced waves are seen primarily on the dayside consistent with previous observations of plasmaspheric hiss [*Meredith et al.*, 2004]. In the outer region, 6 < L^* < 10, the enhanced waves extend from the premidnight sector through dawn into the postnoon sector consistent with previous observations of the MLT dependence of whistler mode chorus [*Li et al.*, 2011; *Meredith et al.*, 2012]. At higher frequencies (Figures 1i, 1e, and 1a), the equatorial plasmaspheric hiss remains confined to the dayside and becomes less intense, while the equatorial chorus moves to lower L^* and also becomes less intense. At midlatitudes, 15° < $|\lambda_m|$ < 30° (Figures 1b, 1f, 1j, and 1n), plasmaspheric hiss is also most intense at low frequencies on the dayside. In contrast, the chorus activity mostly disappears on the nightside while remaining strong in the prenoon sector (06:00–12:00 MLT). At higher midlatitudes, 30° < $|\lambda_m|$ < 45° (Figures 1c, 1g, 1k, and 1o), the plasmaspheric hiss and chorus power weaken before ultimately merging and intensifying at higher latitudes, 45° < $|\lambda_m|$ < 60° (Figures 1d, 1h, 1l, and 1p), predominantly in the prenoon sector.

3.2. Latitudinal Distribution

[8] The global distribution of waves in the plasmaspheric hiss frequency range during active conditions (AE > 100 nT)

on the dayside is shown as a function of frequency band and magnetic local time in the meridional plane in Figure 2. The data have again been averaged over both hemispheres into bins of width $0.2L^*$ and are thus symmetric about the magnetic equator. Dipole field lines and lines of constant magnetic latitude are included to help visualize the behavior of the wave intensities as a function of L^* and λ_m. The average intensities are shown in the large panels and the corresponding sampling distributions in the small panels. The strongest plasmaspheric hiss emissions are seen in the frequency range 200–500 Hz within ±20° of the geomagnetic equator in the region $2 < L^* < 4$ across the whole of the dayside (Figures 2m, 2n, 2o, and 2p). Most importantly, chorus emissions extend to high latitudes in the prenoon sector (first and second columns from left) and ultimately gain access into the plasmasphere [*Bortnik et al.*, 2008]. The chorus source region moves closer to the Earth with increasing frequency ranging from $L^* = 6$–10 in the frequency range 200–500 Hz to $L^* = 4$–5 in the frequency range 2000–3000 Hz. The source chorus power tends to maximize at low and high latitudes and is consistent with theoretical predictions based on ray tracing [*Bortnik et al.*, 2011a, 2011b].

4. Discussion

[9] Previous ray tracing studies have suggested that whistler mode chorus may propagate into the plasmasphere and form the embryonic source of plasmaspheric hiss [e.g., *Bortnik et al*., 2008, 2011a]. Our global statistical observations provide evidence that chorus waves can access the plasmasphere primarily in the prenoon sector but only at high latitudes and not near the magnetic equator. The satellite observations are largely consistent with ground observations of chorus which report the strongest amplitudes near dawn with weaker amplitudes at later local times due to propagation losses through the ionosphere [*Smith et al.*, 2010]. Chorus can propagate from the equatorial region to high latitudes on the dayside due to the absence of strong Landau damping by suprathermal electrons [*Bortnik et al.*, 2007]. In contrast, larger suprathermal electron fluxes on the nightside lead to strong Landau damping which tends to confine chorus to the equatorial region at night [*Bortnik et al*., 2007].

[10] Figure 3 shows the average spectral intensity as a function of frequency and L^* in the equatorial region in the prenoon sector, where the waves have most favorable access to the plasmasphere. The results of the statistical study are shown in Figure 3a, and the simulation results of the plasmaspheric hiss spectrum based on ray tracing from a chorus source are shown in Figure 3b, reproduced and rescaled from *Chen et al.* [2012c]. From top to bottom, the white dotted lines represent $0.3f_{ce}$, $0.1f_{ce}$, and f_{lhr}, respectively, where f_{ce} is the electron gyrofrequency and f_{lhr} is the lower hybrid resonance frequency. At higher frequencies, the chorus source moves to lower L^* consistent with a source from chorus waves in the range 0.1–$0.3f_{ce}$ [*Chen et al.*, 2012b]. There is a clear and distinct gap between the chorus emissions observed outside the plasmapause and the plasmaspheric hiss emissions observed inside (Figures 1i, 1m, 2i, 2m, and 3a), and this is a key prediction of ray tracing modeling from a chorus source (Figure 3b) [*Bortnik et al.*, 2008, 2011b; *Chen et al*., 2012a, 2012b, 2012c]. We note

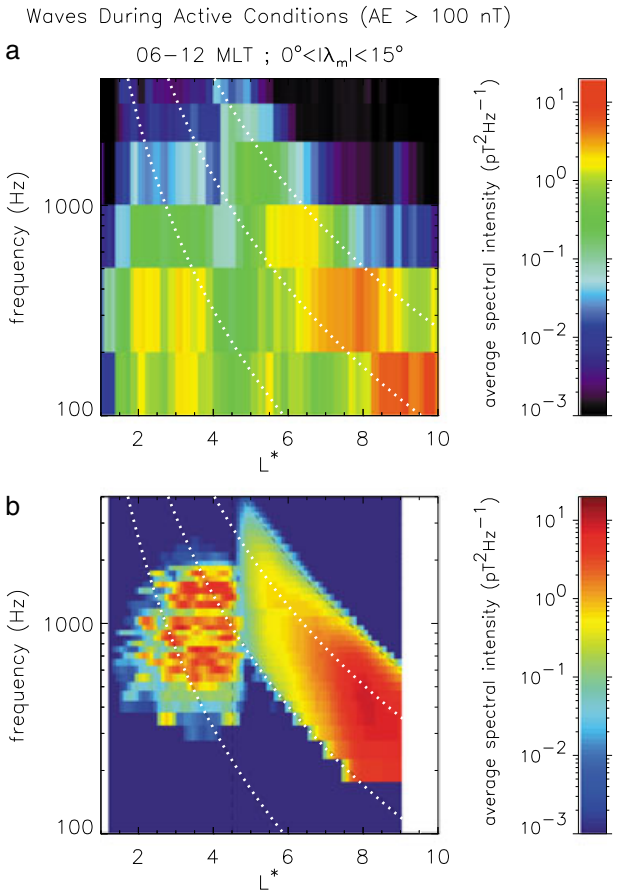

Figure 3. (a) Plot of the observed wave spectral intensity as a function of frequency and L^* in the prenoon sector in the equatorial region. (b) Plot of the simulated wave spectral intensity as a function of frequency and L^* reproduced and rescaled from *Chen et al.* [2012c]. (from top to bottom) The dotted white lines represent $0.3f_{ce}$, $0.1f_{ce}$, and f_{lhr}, respectively.

that the simulated plasmaspheric hiss bandwidth falls into higher frequencies than the observed bandwidth, and this is most likely due to the fact that the electron distribution used to calculate wave growth rates inside the plasmasphere in the simulation is from a single pass of a "typical event" on THEMIS [*Chen et al.*, 2012c], whereas the statistical results of the plasmaspheric hiss spectrum shown here are for average conditions.

[11] There is evidence for enhanced plasmaspheric hiss power from the entry point in the prenoon sector all the way round to 18:00 MLT (Figure 1m). This supports the idea of entry from a localized region in the prenoon sector followed by meridional [*Bortnik et al.*, 2011b] and off-meridional [*Chen et al.*, 2009] propagation. For example, recent 3-D ray tracing simulations of VLF waves in a storm time geospace environment show that off-meridian propagation can be very effective in the postnoon sector due to a strong azimuthal plasma density gradient, enabling rays to propagate eastward where they can potentially explain duskside plasmaspheric hiss emissions [*Chen et al.*, 2009]. Nightside chorus, which is tightly confined to the equatorial region [e.g., *Meredith et al.*, 2012], cannot propagate to high latitudes and is not the source of the weak nightside plasma-

spheric hiss. These weaker emissions may also be explained by off-meridian propagation from a dayside chorus source [*Chen et al.*, 2009]. The theory can thus account for the observed day-night asymmetry which cannot be explained by a lightning source.

[12] Our multisatellite observational results provide compelling statistical evidence for chorus as the embryonic source of plasmaspheric hiss and clearly illustrate the route by which chorus evolves into plasmaspheric hiss, with a chorus source in the prenoon sector which evolves into plasmaspheric hiss throughout the plasmasphere at all local times. Understanding the source of plasmaspheric hiss enables ray tracing from a chorus source outside the plasmasphere to model plasmaspheric hiss inside the plasmasphere. This is important because a better understanding of the properties of plasmaspheric hiss, in particular its wave normal angle distribution which is rarely available, will improve physics-based space weather forecasts [*Horne et al.*, 2013] and help protect satellites from radiation hazards. These improved forecasts will be particularly relevant for future satellite missions designed to operate in the slot region, such as the O3b next-generation satellite network [www.o3bnetworks.com], the first four satellites of which are scheduled for launch in June 2013.

5. Conclusions

[13] We have conducted a global statistical survey of waves in the plasmaspheric hiss frequency range during active conditions using plasma wave data from six satellites. Our main conclusions are as follows:

[14] 1. During active conditions ($AE > 100$ nT), plasmaspheric hiss is most intense on the dayside in the region $2 < L^* < 4$.

[15] 2. In the prenoon sector, intense chorus extends to high latitudes where it may access the plasmasphere and form the embryonic source of plasmaspheric hiss.

[16] 3. The source region of the chorus propagating to higher latitudes is frequency dependent with lower frequencies coming further from the planet, consistent with a chorus source with frequencies in the range $0.1–0.3f_{ce}$.

[17] 4. A clear gap is observed in the prenoon sector in the equatorial region between the plasmaspheric hiss inside the plasmapause and the chorus outside the plasmapause, as predicted by ray tracing studies treating chorus as the source of plasmaspheric hiss.

[18] Our results confirm the new theory and have a general applicability since the process may also operate on other planets with magnetic fields [e.g., *Wang et al.*, 2008].

[19] **Acknowledgments.** We thank K. H. Yearby and V. Angelopoulos for provision of data from Double Star TC-1 and THEMIS, respectively. We acknowledge the CDAWeb and Cluster Active Archive Web sites for provision of data from DE1 and Cluster, respectively. We also acknowledge NSF grant AGS0840178 and NASA grants NNX11AR64G and NNX11AD75G. The research leading to these results has received funding from the European Union Seventh Framework Programme (FP7/2007–2013) under grant agreement 262468 and the Natural Environment Research Council.

[20] The Editor thanks two anonymous reviewers for their assistance in evaluating this paper.

References

Bortnik, J., R. M. Thorne, and N. P. Meredith (2007), Modeling the propagation characteristics of chorus using CRRES suprathermal electron fluxes, *J. Geophys. Res.*, *112*, A08204, doi:10.1029/2006JA012237.

Bortnik, J., R. M. Thorne, and N. P. Meredith (2008), The unexpected origin of plasmaspheric hiss from discrete chorus emissions, *Nature*, *452*, 62–66, doi:10.1038/nature06741.

Bortnik, J., W. Li, R. M. Thorne, V. Angelopoulos, C. Cully, J. Bonnell, O. Le Contel, and A. Roux (2009), An observation linking the origin of plasmaspheric hiss to discrete chorus emissions, *Science*, *324*(5928), 775–778, doi:10.1126/science.1171273.

Bortnik, J., L. Chen, W. Li, R. M. Thorne, and R. B. Horne (2011a), Modeling the evolution of chorus waves into plasmaspheric hiss, *J. Geophys. Res.*, *116*, A08221, doi:10.1029/2011JA016499.

Bortnik, J, L. Chen, W. Li, N. P. Meredith, and R. B. Horne (2011b), Modelling the wave power distribution and characteristics of plasmaspheric hiss, *J. Geophys. Res.*, *116*, A12209, doi:10.1029/2011JA016862.

Chen, L., J. Bortnik, R. M. Thorne, R. B. Horne, and V. K. Jordanova (2009), Three-dimensional ray tracing of VLF waves in a magnetospheric environment containing a plasmaspheric plume, *Geophys. Res. Lett.*, *36*, L22101, doi:10.1029/2009GL040451.

Chen, L., J. Bortnik, W. Li, R. M. Thorne, and R. B. Horne (2012a), Modeling the properties of plasmaspheric hiss: 1. Dependence on chorus wave emission, *J. Geophys. Res.*, *117*, A05201, doi:10.1029/2011JA017201.

Chen, L., J. Bortnik, W. Li, R. M. Thorne, and R. B. Horne (2012b), Modeling the properties of plasmaspheric hiss: 2. Dependence on the plasma density distribution, *J. Geophys. Res.*, *117*, A05202, doi:10.1029/2011JA017202.

Chen, L., W. Li, J. Bortnik, and R. M. Thorne (2012c), Amplification of whistler-mode hiss inside the plasmasphere, *Geophys. Res. Lett.*, *39*, L08111, doi:10.1029/2012GL051488.

Church, S., and R. M. Thorne (1983), On the origin of plasmaspheric hiss: Ray path integrated amplification, *J. Geophys. Res.*, *88*, 7941–7957.

Horne, R. B., S. A. Glauert, N. P. Meredith, D. Boscher, V. Maget, D. Heynderickx, and D. Pitchford (2013), Space weather impacts on satellites and forecasting the Earth's electron radiation belts with SPACECAST, *Space Weather*, *11*, 169–186, doi:10.1002/swe.20023.

Li, W., J. Bortnik, R. M. Thorne, and V. Angelopoulos (2011), Global distribution of wave amplitudes and wave normal angles of chorus waves using THEMIS wave observations, *J. Geophys. Res.*, *116*, A12205, doi:10.1029/2011JA017035.

Lyons, L. R., and R. M. Thorne (1973), Equilibrium structure of radiation belt electrons, *J. Geophys. Res.*, *78*, 2142–2149.

Meredith, N. P., R. B. Horne, R. M. Thorne, D. Summers, and R. R. Anderson (2004), Substorm dependence of plasmaspheric hiss, *J. Geophys. Res.*, *109*, A06209, doi:10.1029/2004JA010387.

Meredith, N. P., R. B. Horne, M. A. Clilverd, D. Horsfall, R. M. Thorne, and R. R. Anderson (2006a), Origins of plasmaspheric hiss, *J. Geophys. Res.*, *111*, A09217, doi:10.1029/2006JA011707.

Meredith, N. P., R. B. Horne, S. A. Glauert, R. M. Thorne, D. Summers, J. M. Albert, and R. R. Anderson (2006b), Energetic outer zone electron loss timescales during low geomagnetic activity, *J. Geophys. Res.*, *111*, A05212, doi:10.1029/2005JA011516.

Meredith, N. P., R. B. Horne, S. A. Glauert, and R. R. Anderson (2007), Slot region electron loss timescales due to plasmaspheric hiss and lightning generated whistlers, *J. Geophys. Res.*, *112*, A08214, doi:10.1029/2006JA012413.

Meredith, N. P., R. B. Horne, S. A. Glauert, D. N. Baker, S. G. Kanekal, and J. M. Albert (2009), Relativistic electron loss timescales in the slot region, *J. Geophys. Res.*, *114*, A03222, doi:10.1029/2008JA013889.

Meredith, N. P., R. B. Horne, A. Sicard-Piet, D. Boscher, K. H. Yearby, W. Li, and R. M. Thorne (2012), Global model of lower band and upper band chorus from multiple satellite observations, *J. Geophys. Res.*, *117*, A12209, doi:10.1029/2012JA017978.

Nemec, F., O. Santolík, K. Gereová, E. Macúšová, Y. de Conchy, and N. Cornilleau-Wehrlin (2005), Initial results of a survey of equatorial noise emissions observed by the Cluster spacecraft, *Planet. Space Sci.*, *53*, 91–298.

Olson, W. P., and K. Pfitzer (1977), Magnetospheric magnetic field modelling annual scientific report, *AFOSR Contract F44620-75-c-0033.*

Roederer, J. G. (1970), *Dynamics of Geomagnetically Trapped Radiation*, 166 pp., Springer-Verlag, New York.

Smith, A. J., R. B. Horne, and N. P. Meredith (2010), The statistics of natural ELF/VLF waves derived from a long continuous set of ground-based observations at high latitude, *J. Atmos. Sol. Terr. Phys.*, *72*, 463–475.

Smith, E. J., A. M. A. Frandsen, B. T. Tsurutani, R. M. Thorne, and K. W. Chan (1974), Plasmaspheric hiss intensity variations during magnetic storms, *J. Geophys. Res.*, *79*(16), 2507–2510.

Sonwalkar, V. S., and U. S. Inan (1989), Lightning as an embryonic source of VLF hiss, *J. Geophys. Res.*, *94*, 6986–6994.

Summers, D., B. Ni, and N. P. Meredith (2007), Timescales for radiation belt electron acceleration and loss due to resonant wave-particle interactions: 2. Evaluation for VLF chorus, ELF hiss, and electromag-

netic ion cyclotron waves, *J. Geophys. Res.*, *112*, A04207, doi:10.1029/2006JA011993.

Summers, D., B. Ni, N. P. Meredith, R. B. Horne, R. M. Thorne, M. B. Moldwin, and R. R. Anderson (2008), Electron scattering by whistler-mode ELF hiss in plasmaspheric plumes, *J. Geophys. Res.*, *113*, A04219, doi:10.1029/2007JA012678.

Thorne, R. M., E. J. Smith, R. K. Burton, and R. E. Holzer (1973), Plasmaspheric hiss, *J. Geophys. Res.*, *78*(10), 1581–1596.

Thorne, R. M., E. J. Smith, K. J. Fiske, and S. R. Church (1974), Intensity variation of ELF hiss and chorus driving isolated substorms, *Geophys. Res. Lett.*, *1*(5), 193–196.

Tsurutani, B. T., B. J. Falkowski, O. P. Verkhoglyadova, J. S. Pickett, O. Santolík, and G. S. Lakhina (2012), Dayside ELF electromagnetic wave survey: A Polar statistical study of chorus and hiss, *J. Geophys. Res.*, *117*, A00L12, doi:10.1029/2011JA017180.

Wang, K., R. M. Thorne, and R. B. Horne (2008), Origin of Jovian hiss in the extended Io torus, *Geophys. Res. Lett.*, *35*, L16105, doi:10.1029/2008GL034636.

Wang, C., Q. Zong, F. Xiao, Z. Su, Y. Wang, and C. Yue (2011), The relations between magnetospheric chorus and hiss inside and outside the plasmasphere boundary layer: Cluster observation, *J. Geophys. Res.*, *116*, A07221, doi:10.1029/2010JA016240.